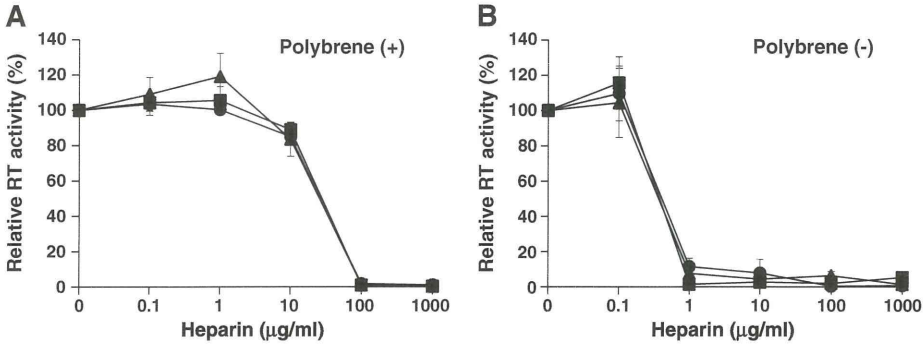


**Fig. 5.** Effects of polybrene on inhibitory activities of heparin against MLV infection. F- (triangle), A8 (circle), and PVC-211 (square) MLVs were pre-incubated with various concentrations of heparin for 1 h at 37 °C in the absence of polybrene. Then, the virus–heparin mixture was inoculated onto NIH 3T3 cells in the presence of 10 μg/ml polybrene (A) or in its absence (B). After incubation for 1 h at 37 °C, the cells were washed three times with FCS-free DMEM and fresh culture medium was added. After 96 h, virion-associated RT activity in the culture supernatants was measured by an RT assay as described in the Materials and methods section. The mean values of 4 independent experiments and SEM are shown.

infection. Third, we cannot exclude the possibility that heparin might affect viral replication steps except for attachment. Although we used VSV-pseudotyped viruses carrying Env for the inhibition assay against viral infection, the assay did not distinguish rigorously between viral attachment and alternative steps in infection, such as entry and gene expression. Therefore, heparin might not only influence viral attachment but also entry and gene expression, with the result that the $ID_{50}$ values for viral infection are similar among the viruses despite the fact that they carry different Envs.

Heparin is a highly sulfated polysaccharide with a negative charge and its most common disaccharide unit is composed of 2-*O*-sulfated iduronic acid and 6-*O*-sulfated, *N*-sulfated glucosamine (Fig. 1E). Sulfation of heparan sulfate, which is structurally related to heparin, is thought to play an important role in its biological activity such as FGF signaling and its ability to act as an entry receptor for herpes simplex virus type 1 (Capila and Linhardt, 2002; Copeland et al., 2008; Shukla et al., 1999; Xia et al., 2002; Ye et al., 2001). It has also been shown that the chemical structure of the carbohydrate unit constituting the GAG backbone is an important determinant for the ability of the GAG to inhibit retroviral infection (Jinno-Oue et al., 2001; Walker et al., 2002). By comparing the effects of heparin and dNS-H, Jinno-Oue et al. (2001) concluded that *N*-sulfation of GAG is important for the effects on infectivity of ecotropic MLVs. In this study, NA-H, which has diminished *N*-sulfation, and dNS-H, which completely lacks *N*-sulfation, were shown to be less effective than heparin in inhibiting infection of NIH 3T3 cells by pseudotyped viruses carrying ecotropic MLV Env (Fig. 3 and Table 2). We have, therefore, confirmed that *N*-sulfation of GAG plays an important role in the inhibition of ecotropic MLV infection. In addition, NAdOS-H, which has markedly diminished *N*-sulfation and completely lacks *O*-sulfation, did not significantly alter infectivity of pseudotyped viruses on NIH 3T3 cells (Fig. 3). Comparison of dNS-H and NAdOS-H strongly suggests that the *O*-sulfate groups of GAG are also required for the inhibitory effects on MLV infection. Intriguingly, the results of the SPR analysis indicated that NAdOS-H, which failed to inhibit ecotropic MLV infection, binds to F-, A8-, and PVC-211-Env at levels comparable to those of dNS-H, which unequivocally exhibited inhibitory effects on viral infection. Therefore, binding of GAG to the viral Env may be essential, but not sufficient, for inhibition of Env-dependent MLV attachment to the cell surface. Previous studies have highlighted the importance of the *O*-sulfate group of heparin for its inhibitory activities against infection by pseudorabies virus (Trybala et al., 1996), herpes simplex virus (Trybala et al., 2000), and HIV (Rider et al., 1994). In contrast, *N*-sulfation of heparin is required for inhibition of respiratory syncytial virus infection (Hallak et al., 2000). The results from the

**Table 3**
$ID_{50}$ of heparin against infection of MLVs into NIH 3T3 cells in the presence or absence of polybrene.

| Polybrene | Viruses | | |
|---|---|---|---|
| | F | A8 | PVC-211 |
| Present | 44.4 ± 6.7 | 47.9 ± 0.8 | 49.6 ± 2.2 |
| Absent | 0.56 ± 0.08[a] | 0.61 ± 0.10[a] | 0.60 ± 0.05[a] |

$ID_{50}$ values (μg/ml) were calculated from the data shown in Fig. 5. The mean values (and SEMs) of 4 independent experiments are shown. Statistical comparison was performed using the t test.

[a] $P < 0.001$ vs presence of polybrene in each virus.

| Position | Amino Acid F | A8 | PVC-211 | Structural element |
|---|---|---|---|---|
| -28 | Pro | Ser | Ser | |
| 1 | Ala | Val | Ala | RBD |
| 40 | Val | Asp | Asp | RBD |
| 61 | Gln | Arg | Arg | RBD-VRA |
| 79 | Ser | Asn | Asn | RBD-VRA |
| 80 | Ser | Arg | Arg | RBD-VRA |
| 84 | Ser | Ser | Ala | RBD-VRA |
| 116 | Glu | Gly | Gly | RBD-VRA |
| 129 | Glu | Glu | Lys | RBD-VRC |
| 152 | Val | Ala | Ala | RBD |
| 172 | Ser | Asn | Asn | RBD-VRB |
| 175 | Val | Ala | Ala | RBD-VRB |
| 203 | Thr | Ile | Ile | RBD |
| 216 | Arg | Gln | Gln | RBD |
| 227 | Arg | Lys | Lys | RBD |
| 249 | Leu | Phe | Phe | |
| 251 | Arg | Leu | Leu | |
| 263 | Pro | Ser | Ser | |
| 277 | Thr | Ala | Ala | |
| 319 | Gly | Ala | Ala | |
| 344 | Val | Ala | Ala | |
| 345 | Ala | Gly | Gly | |
| 358 | Arg | Gln | Gln | |
| 379 | Ile | Thr | Thr | |
| 380 | Asp | Gly | Gly | |
| 390 | Thr | Ala | Ala | |
| 393 | Thr | Met | Met | |
| 642 | End | Gln | Gln | |

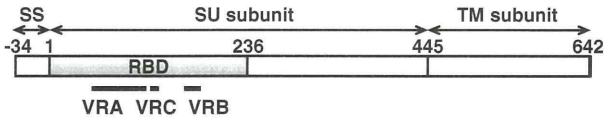


**Fig. 6.** Amino acid sequences of F-, A8-, and PVC-211-Env. A schematic diagram of the Env precursor polyprotein is shown at the bottom. SS: signal sequence; SU: surface protein; TM: transmembrane protein; RBD: receptor-binding domain (Fass et al., 1997); VRA: variable region A; VRB: variable region B; VRC: variable region C. The N-terminal amino acid of the SU is numbered as 1.

earlier studies and from here suggest that different types of sulfate groups are required for the inhibitory activities of heparin against different viruses, and that the anti-viral activity of heparin does not depend simply on negative charge density but involves particular structures, notably sulfation patterns.

Although the interaction between Env and CAT-1, the receptor molecule for MLV, appears to be required for membrane fusion and entry of the viral capsid, it has been reported that initial attachment of MLV to the cell surface can take place in a receptor-independent manner (Guibinga et al., 2002; Pizzato et al., 1999; Walker et al., 2002). Heparan sulfate on the cell surface was proposed as a candidate cell surface molecule for MLV attachment (Batra et al., 1997; Guibinga et al., 2002; Jinno-Oue et al., 2001; Le Doux et al., 1996, 1999; Masuda et al., 1997; Walker et al., 2002). The SPR analyses carried out in the present study also suggest that heparan sulfate on the cell surface is involved in MLV attachment as we found that heparin could bind directly to the Env of MLV. The exact role(s) of the cell surface heparan sulfate in MLV infection is still unknown; nevertheless,

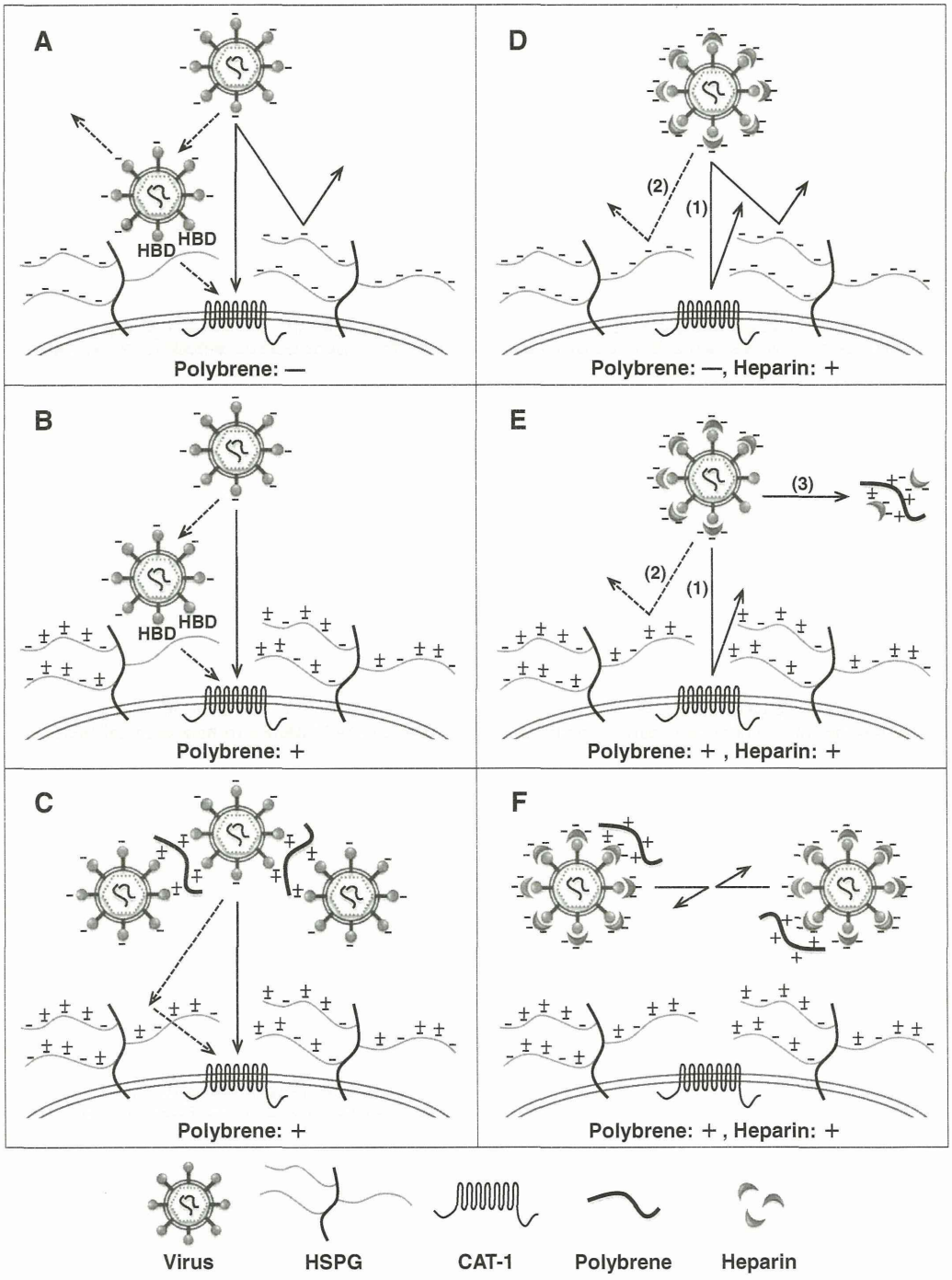


**Fig. 7.** Schematic diagrams of possible mechanisms of attachment of MLV to cells and of the inhibition of attachment by heparin. These various possibilities are described in detail in the Discussion section. CAT-1: cationic amino acid transporter 1 as the specific receptor for ecotropic MLV; HSPG: heparan sulfate proteoglycan.

we suggest a possible model for its behavior in Fig. 7. In this model, heparan sulfate on the cell surface is envisaged as a route for viral infection. The viral particles first bind to heparan sulfate via the HBD of Env and the increase in concentration of viral particles on the cell surface then raises the probability of interaction with CAT-1. On the cell surface, CAT-1 is covered by long chains of heparan sulfate that have a large net negative charge. In the absence of polybrene, it is difficult for viral particles with a negative charge to approach CAT-1 and/or heparan sulfate on the cell surface due to electrostatic repulsion (Fig. 7A). MLV infections are usually carried out in the presence of cationic polymers, such as polybrene to enhance infection, because the infectivity of MLV is very low in the absence of polybrene (Davis et al., 2002). Polybrene appears to enhance the infectivity of MLVs through various possible mechanisms, and some of these have been identified in previous studies. Initially, the positive charge of polybrene might neutralize the negative charge on the cell surface, facilitating access of the viral particles to CAT-1 and/or heparan sulfate on the cell surface (Fig. 7B) (Davis et al., 2004). A second possibility is that polybrene might cause the viral particles to form aggregates that have easier access to the cell surface (Fig. 7C) (Davis et al., 2004; Landazuri and Le Doux, 2004). Based on these putative mechanisms, how might heparin inhibit infection by ecotropic MLV? It is possible that heparin binds to a region near the RBD of Env and sterically or electrostatically blocks interaction between Env and CAT-1 (arrow (1) in Figs. 7D and E). A second possibility is that heparin binds to HBD of Env and that viral particles covered with heparin cannot bind to heparan sulfate on the cell surface (arrow (2) in Figs. 7D and E). Alternatively, viral particles bearing heparin have a large net negative charge and might fail to access the cell surface due to electrostatic repulsion. A final possibility is that polybrene might not be able to aggregate heparin-covered viral particles that bear large negative charges, and this might make access to the cell surface less efficient (Fig. 7F). The $ID_{50}$ values of heparin for F-, A8, and PVC-211 MLVs were lower in the absence of polybrene than in its presence (Fig. 5 and Table 3). In the absence of polybrene, the negative charge of cell surface molecules is not neutralized. Therefore, it is possible that the repulsion between viral particles bearing heparin and cell surface molecules with a negative charge is stronger in the absence of polybrene than in its presence (Figs. 7D and E). As a result, heparin is able to inhibit viral infection effectively in the absence of polybrene. Alternatively, in the presence of polybrene, the part of the heparin molecule that normally binds to viral particles might instead bind with polybrene (arrow (3) in Fig. 7E), with the consequence that a relatively large amount of heparin is required for inhibition of viral infection.

## Materials and methods

### *Reagents*

Heparin (H4784), *N*-acetylheparin (A8036) (NA-H), de-*N*-sulfated heparin (D4776) (dNS-H), and *N*-acetyl-de-*O*-sulfated heparin (A6039) (NAdOS-H) were obtained from Sigma. Heparin obtained from Nacalai Tesque was used in the SPR analysis.

### *Cells and viruses*

NIH 3T3 cells were grown in Dulbecco's modified Eagle's medium (DMEM) containing 10% fetal calf serum (FCS). *Mus dunni* cells were grown in RPMI1640 medium containing 10% FCS. 293T cells were grown on DMEM containing 5% FCS.

Infectious DNA clones of neuropathogenic A8 (Takase-Yoden and Watanabe, 1997; Watanabe and Takase-Yoden, 1995) (database ID: D88386) and PVC-211 MLVs (Kai and Furuta, 1984; Masuda et al., 1992) (database ID: M93134.1) and non-neuropathogenic F-MLV clone 57 (Oliff et al., 1980) (database ID: X02794) were described previously. NIH 3T3 cells were transfected with each DNA clone, and culture supernatants of the virus-producing cells were harvested and stored at −80 °C as stock viruses. Virus titers were determined by a focal immunoassay on *Mus dunni* cells in the presence of 10 μg/ml polybrene as described previously (Czub et al., 1991).

### *Assay of viral reverse transcriptase*

Culture supernatants of the virus-producing cells were centrifuged at 5000 rpm for 5 min at 4 °C. To disrupt the viral particles, 10 μl of the supernatant was mixed with 14 μl of an aqueous solution of 7 mM Tris–HCl (pH7.6), 70 mM NaCl, 0.7 mM ethylenediaminetetraacetic acid (EDTA), and 0.03% Triton X-100. The mixture was then mixed with 16 μl of an aqueous solution of 125 mM Tris–HCl (pH7.6), 150 mM NaCl, 25 mM dithiothreitol, 2.5 mM $MnCl_2$, 250 μg/ml Poly(A) x $(dT)_{15}$ (Roche Diagnostics), and $^3$H-TTP (1 μCi), and incubated for 1 h at 37 °C (Robert-Guroff et al., 1977). The reaction was stopped by addition of 1 μl 0.5 M EDTA, and incorporated radioactivity was determined as described previously (Tamura and Takano, 1978).

### *VSV based-pseudotyped viruses*

Recombinant VSV, VSVΔG*/GFP-G, was kindly provided by Dr. Whitt. The virus carries the jellyfish GFP gene in place of the viral G protein gene, and its G protein is supplemented by a separate expression vector (Takada et al., 1997). The *env* genes of F-, A8, and PVC-211 MLVs were each cloned into a pCAGGS expression vector (pCAGGS-F-env, pCAGGS-A8-env, and pCAGGS-PVC-211-env, respectively). pCAGGS was kindly provided by Dr. Miyazaki, and transfected into 293T cells. To prepare VSV-based pseudotyped viruses, the cells were infected 24 h after transfection with VSVΔG*/GFP-G at an MOI of 10. After 12 h, the supernatant of each culture was replaced with fresh medium, and the cells were cultured for an additional 12 h. The culture supernatants were then collected, passed through a 0.22 μm pore size filter and stored at −80 °C as VSV-based pseudotyped viruses: VSV/F-Env, VSV/A8-Env, and VSV/PVC-211-Env, carrying Env of F-, A8, and PVC-211 MLVs, respectively. 293T cells that had not been transfected with the Env expression vector were also infected with VSVΔG*/GFP-G for preparing VSV viruses-like particles lacking Env (VSV/ΔEnv). To measure viral titer, NIH 3T3 cells were infected with each of the pseudotyped viruses in the presence of 10 μg/ml of polybrene and, at 16 h post-infection, GFP-positive cells were counted by flow cytometry.

### *FACS analysis*

Cells were harvested and washed twice with FACS buffer (phosphate-buffered saline [PBS] containing 0.25% FCS, 0.25% horse serum, and 0.1% sodium azide). Then, the cells were suspended in FACS buffer and analyzed for GFP expression using a FACSAria Cell Sorter (BD Biosciences).

### *Immunoblot analysis*

Western blot analysis was performed on 293T cells transfected with pCAGGS-F-env, pCAGGS-A8-env, or pCAGGS-PVC-211-env vectors, or with virions of VSV/F-Env, VSV/A8-Env, VSV/PVC-211-Env, VSV/ΔEnv; Mock transfected cells were used as a control. Cells were harvested at 48 h after transfection with the *env* expression vector. Cells were washed with PBS and then lysed with 2% sodium dodecyl sulfate (SDS) and 0.5 mM phenylmethylsulfonyl fluoride (PMSF) in PBS at 100 °C for 5 min. Nucleic acid was mechanically sheared using a syringe with a 22-gauge needle. A 1 ml aliquot of each virus supernatant, containing the $2\times10^5$ infectious units, was then subjected to ultracentrifugation at 30,000 rpm in a Beckman SW 41 Ti

rotor at 4 °C for 2 h to purify the virions. Precipitates containing virions were suspended in PBS. Sample buffer (5×) containing SDS, DTT, glycerol, and bromophenol blue in Tris–HCl (pH 6.8) was added to the cell lysate or the virion suspension. After boiling for 5 min, the lysates were loaded on a 10% SDS-polyacrylamide gel and electrophoresed. The proteins were then transferred to an Immobilon P membrane (Millipore) by electroblotting. To detect the Env protein, goat anti-Rauscher MLV gp70 (Quality Biotech Incorporated-Resource Laboratory) was used. Actin was detected using rabbit anti-beta-actin (Santa Cruz Biotechnology) as a loading control. Horseradish peroxidase-conjugated anti-goat IgG antibody and horseradish peroxidase-conjugated anti-rabbit IgG antibody (Santa Cruz Biotechnology) were used as secondary antibodies. The membrane was developed with ECL plus reagents (GE Healthcare). Band images were captured with LAS-3000 (FUJIFILM).

### *Preparation of VSV based-pseudotyped viruses for SPR analysis*

Suspensions of VSV/F-Env, VSV/A8-Env, or VSV/PVC-211-Env ($1\times10^6$ infectious units) were made up to 5 ml by adding fresh culture medium; they were then dialyzed in a cellulose tube (EIDIA Co., Ltd.) against 200× PBS (v/v) for 24 h at 4 °C, with the outer solution refreshed four times. Then, the solutions were fixed with 2% paraformaldehyde (PFA) buffered with 0.12 M phosphate (pH7.3). To remove the PFA, the solutions were dialyzed in a cellulose tube against 200× PBS (v/v) for 24 h at 4 °C, with the outer solution refreshed four times. Then, the solutions were concentrated at 4 °C to 0.5 ml ($2\times10^6$ infectious units/ml) using an Amicon Ultra-15 100 K Centrifugal Filter Device (Millipore) and stored at −80 °C until use. For the negative control, we used an aliquot of the culture supernatant of VSV/ΔEnv-producing 293T cells; for the Mock control, we used an aliquot of the culture supernatant of 293T cells. For both controls, the aliquot was equivalent in volume to the sample from the culture supernatant of VSV/Env-producing cells, which contained $1\times10^6$ infectious units, and was treated in the same manner as above.

### *SPR analysis*

Heparin, NAdOS-H and dNS-H were dialyzed against distilled water using an MWCO3500 membrane (SpectroPore), lyophilized, and then conjugated with an f-mono linker molecule to prepare the ligand conjugate as previously described (Sato et al., 2009; Suda et al., 2006). To prepare the Sugar Chip with immobilized ligand, the surface of a gold-coated chip (SUDx-Biotec) was oxidatively washed with UV ozone cleaner (Structure Probe Inc.) for 20 min and then immersed in 1 μM of the ligand conjugate dissolved in 50% (v/v) methanol solution overnight at room temperature with gentle agitation. The Sugar Chip was washed sequentially with water, 0.05% Tween 20, and water and dried at room temperature. For the SPR analysis, the Sugar Chip was set on a prism with refraction oil (nD = 1.518, Cargill Laboratories Inc.) in an SPR apparatus (SPR670M, Moritex). The SPR measurements were performed at room temperature according to the manufacturer's instructions, using PBS containing 0.05% Tween 20 as the running buffer at a flow rate of 15 μl/min.

## Acknowledgments

We thank Dr. M. A. Whitt for providing VSVΔG*/GFP-G, and Dr. J. Miyazaki for providing pCAGGS. This work was supported in part by funding from MEXT (Ministry of Education, Culture, Sports, Science and Technology), the Matching Fund for Private Universities, S0901015, 2009–2014.

## References

Albritton, L.M., Tseng, L., Scadden, D., Cunningham, J.M., 1989. A putative murine ecotropic retrovirus receptor gene encodes a multiple membrane-spanning protein and confers susceptibility to virus infection. Cell 57, 659–666.

Batra, R.K., Olsen, J.C., Hoganson, D.K., Caterson, B., Boucher, R.C., 1997. Retroviral gene transfer is inhibited by chondroitin sulfate proteoglycans/glycosaminoglycans in malignant pleural effusions. J. Biol. Chem. 272, 11736–11743.

Capila, I., Linhardt, R.J., 2002. Heparin–protein interactions. Angew. Chem. 41, 391–412.

Cardin, A.D., Weintraub, H.J., 1989. Molecular modeling of protein–glycosaminoglycan interactions. Arteriosclerosis 9, 21–32.

Copeland, R., Balasubramaniam, A., Tiwari, V., Zhang, F., Bridges, A., Linhardt, R.J., Shukla, D., Liu, J., 2008. Using a 3-O-sulfated heparin octasaccharide to inhibit the entry of herpes simplex virus type 1. Biochemistry 47, 5774–5783.

Crublet, E., Andrieu, J.P., Vives, R.R., Lortat-Jacob, H., 2008. The HIV-1 envelope glycoprotein gp120 features four heparan sulfate binding domains, including the co-receptor binding site. J. Biol. Chem. 283, 15193–15200.

Czub, M., Czub, S., McAtee, F.J., Portis, J.L., 1991. Age-dependent resistance to murine retrovirus-induced spongiform neurodegeneration results from central nervous system-specific restriction of virus replication. J. Virol. 65, 2539–2544.

Davis, H.E., Morgan, J.R., Yarmush, M.L., 2002. Polybrene increases retrovirus gene transfer efficiency by enhancing receptor-independent virus adsorption on target cell membranes. Biophys. Chem. 97, 159–172.

Davis, H.E., Rosinski, M., Morgan, J.R., Yarmush, M.L., 2004. Charged polymers modulate retrovirus transduction via membrane charge neutralization and virus aggregation. Biophys. J. 86, 1234–1242.

Fass, D., Davey, R.A., Hamson, C.A., Kim, P.S., Cunningham, J.M., Berger, J.M., 1997. Structure of a murine leukemia virus receptor-binding glycoprotein at 2.0 angstrom resolution. Science 277, 1662–1666.

Guibinga, G.H., Miyanohara, A., Esko, J.D., Friedmann, T., 2002. Cell surface heparan sulfate is a receptor for attachment of envelope protein-free retrovirus-like particles and VSV-G pseudotyped MLV-derived retrovirus vectors to target cells. Mol. Ther. 5, 538–546.

Hallak, L.K., Spillmann, D., Collins, P.L., Peeples, M.E., 2000. Glycosaminoglycan sulfation requirements for respiratory syncytial virus infection. J. Virol. 74, 10508–10513.

Jinno-Oue, A., Oue, M., Ruscetti, S.K., 2001. A unique heparin-binding domain in the envelope protein of the neuropathogenic PVC-211 murine leukemia virus may contribute to its brain capillary endothelial cell tropism. J. Virol. 75, 12439–12445.

Kai, K., Furuta, T., 1984. Isolation of paralysis-inducing murine leukemia viruses from Friend virus passaged in rats. J. Virol. 50, 970–973.

Kim, J.W., Closs, E.I., Albritton, L.M., Cunningham, J.M., 1991. Transport of cationic amino acids by the mouse ecotropic retrovirus receptor. Nature 352, 725–728.

Krusat, T., Streckert, H.J., 1997. Heparin-dependent attachment of respiratory syncytial virus (RSV) to host cells. Arch. Virol. 142, 1247–1254.

Landazuri, N., Le Doux, J.M., 2004. Complexation of retroviruses with charged polymers enhances gene transfer by increasing the rate that viruses are delivered to cells. J. Gene Med. 6, 1304–1319.

Le Doux, J.M., Morgan, J.R., Snow, R.G., Yarmush, M.L., 1996. Proteoglycans secreted by packaging cell lines inhibit retrovirus infection. J. Virol. 70, 6468–6473.

Le Doux, J.M., Morgan, J.R., Yarmush, M.L., 1999. Differential inhibition of retrovirus transduction by proteoglycans and free glycosaminoglycans. Biotechnol. Prog. 15, 397–406.

Masuda, M., Remington, M.P., Hoffman, P.M., Ruscetti, S.K., 1992. Molecular characterization of a neuropathogenic and nonerythroleukemogenic variant of Friend murine leukemia virus PVC-211. J. Virol. 66, 2798–2806.

Masuda, M., Hanson, C.A., Dugger, N.V., Robbins, D.S., Wilt, S.G., Ruscetti, S.K., Hoffman, P.M., 1997. Capillary endothelial cell tropism of PVC-211 murine leukemia virus and its application for gene transduction. J. Virol. 71, 6168–6173.

Mondor, I., Ugolini, S., Sattentau, Q.J., 1998. Human immunodeficiency virus type 1 attachment to HeLa CD4 cells is CD4 independent and gp120 dependent and requires cell surface heparans. J. Virol. 72, 3623–3634.

Neyts, J., Snoeck, R., Schols, D., Balzarini, J., Esko, J.D., Van Schepdael, A., De Clercq, E., 1992. Sulfated polymers inhibit the interaction of human cytomegalovirus with cell surface heparan sulfate. Virology 189, 48–58.

Oliff, A.I., Hager, G.L., Chang, E.H., Scolnick, E.M., Chan, H.W., Lowy, D.R., 1980. Transfection of molecularly cloned Friend murine leukemia virus DNA yields a highly leukemogenic helper-independent type C virus. J. Virol. 33, 475–486.

Patel, M., Yanagishita, M., Roderiquez, G., Bou-Habib, D.C., Oravecz, T., Hascall, V.C., Norcross, M.A., 1993. Cell-surface heparan sulfate proteoglycan mediates HIV-1 infection of T-cell lines. AIDS Res. Hum. Retroviruses 9, 167–174.

Pizzato, M., Marlow, S.A., Blair, E.D., Takeuchi, Y., 1999. Initial binding of murine leukemia virus particles to cells does not require specific Env-receptor interaction. J. Virol. 73, 8599–8611.

Rider, C.C., Coombe, D.R., Harrop, H.A., Hounsell, E.F., Bauer, C., Feeney, J., Mulloy, B., Mahmood, N., Hay, A., Parish, C.R., 1994. Anti-HIV-1 activity of chemically modified heparins: correlation between binding to the V3 loop of gp120 and inhibition of cellular HIV-1 infection in vitro. Biochemistry 33, 6974–6980.

Robert-Guroff, M., Schrecker, A.W., Brinkman, B.J., Gallo, R.C., 1977. DNA polymerase gamma of human lymphoblasts. Biochemistry 16, 2866–2873.

Sato, M., Ito, Y., Arima, N., Baba, M., Sobel, M., Wakao, M., Suda, Y., 2009. High-sensitivity analysis of naturally occurring sugar chains, using a novel fluorescent linker molecule. J. Biochem. 146, 33–41.

Secchiero, P., Sun, D., De Vico, A.L., Crowley, R.W., Reitz Jr., M.S., Zauli, G., Lusso, P., Gallo, R.C., 1997. Role of the extracellular domain of human herpesvirus 7 glycoprotein B in virus binding to cell surface heparan sulfate proteoglycans. J. Virol. 71, 4571–4580.

Shukla, D., Liu, J., Blaiklock, P., Shworak, N.W., Bai, X., Esko, J.D., Cohen, G.H., Eisenberg, R.J., Rosenberg, R.D., Spear, P.G., 1999. A novel role for 3-O-sulfated heparan sulfate in herpes simplex virus 1 entry. Cell 99, 13–22.

Suda, Y., Arano, A., Fukui, Y., Koshida, S., Wakao, M., Nishimura, T., Kusumoto, S., Sobel, M., 2006. Immobilization and clustering of structurally defined oligosaccharides for sugar chips: an improved method for surface plasmon resonance analysis of protein–carbohydrate interactions. Bioconjug. Chem. 17, 1125–1135.

Takada, A., Robison, C., Goto, H., Sanchez, A., Murti, K.G., Whitt, M.A., Kawaoka, Y., 1997. A system for functional analysis of Ebola virus glycoprotein. Proc. Natl. Acad. Sci. U. S. A. 94, 14764–14769.

Takase-Yoden, S., Watanabe, R., 1997. Unique sequence and lesional tropism of a new variant of neuropathogenic Friend murine leukemia virus. Virology 233, 411–422.

Tamura, T.-A., Takano, T., 1978. A new, rapid procedure for the concentration of C-type viruses from large quantities of culture media: ultrafiltration by diaflo membrane and purification by ficoll gradient centrifugation. J. Gen. Virol. 41, 135–141.

Trybala, E., Bergström, T., Spillmann, D., Svennerholm, B., Olofsson, S., Flynn, S.J., Ryan, P., 1996. Mode of interaction between pseudorabies virus and heparan sulfate/heparin. Virology 218, 35–42.

Trybala, E., Liljeqvist, J.A., Svennerholm, B., Bergström, T., 2000. Herpes simplex virus types 1 and 2 differ in their interaction with heparan sulfate. J. Virol. 74, 9106–9114.

Walker, S.J., Pizzato, M., Takeuchi, Y., Devereux, S., 2002. Heparin binds to murine leukemia virus and inhibits Env-independent attachment and infection. J. Virol. 76, 6909–6918.

Wang, H., Kavanaugh, M.P., North, R.A., Kabat, D., 1991. Cell-surface receptor for ecotropic murine retroviruses is a basic amino-acid transporter. Nature 352, 729–731.

Watanabe, R., Takase-Yoden, S., 1995. Gene expression of neurotropic retrovirus in the CNS. Prog. Brain Res. 105, 255–262.

WuDunn, D., Spear, P.G., 1989. Initial interaction of herpes simplex virus with cells is binding to heparan sulfate. J. Virol. 63, 52–58.

Xia, G., Chen, J., Tiwari, V., Ju, W., Li, J.P., Malmstrom, A., Shukla, D., Liu, J., 2002. Heparan sulfate 3-O-sulfotransferase isoform 5 generates both an antithrombin-binding site and an entry receptor for herpes simplex virus, type 1. J. Biol. Chem. 277, 37912–37919.

Ye, S., Luo, Y., Lu, W., Jones, R.B., Linhardt, R.J., Capila, I., Toida, T., Kan, M., Pelletier, H., McKeehan, W.L., 2001. Structural basis for interaction of FGF-1, FGF-2, and FGF-7 with different heparan sulfate motifs. Biochemistry 40, 14429–14439.

# A more efficient method to generate integration-free human iPS cells

Keisuke Okita[1], Yasuko Matsumura[1], Yoshiko Sato[1], Aki Okada[1], Asuka Morizane[1,2], Satoshi Okamoto[3], Hyenjong Hong[1], Masato Nakagawa[1], Koji Tanabe[1], Ken-ichi Tezuka[4], Toshiyuki Shibata[5], Takahiro Kunisada[4], Masayo Takahashi[1,3], Jun Takahashi[1,2], Hiroh Saji[6] & Shinya Yamanaka[1,7–9]

**We report a simple method, using p53 suppression and nontransforming L-Myc, to generate human induced pluripotent stem cells (iPSCs) with episomal plasmid vectors. We generated human iPSCs from multiple donors, including two putative human leukocyte antigen (HLA)-homozygous donors who match ~20% of the Japanese population at major HLA loci; most iPSCs are integrated transgene-free. This method may provide iPSCs suitable for autologous and allologous stem-cell therapy in the future.**



Genomic integration of transgenes increases the risk of tumor formation and mortality in chimeric and progeny mice derived from induced pluripotent stem cells (iPSCs)[1]. Integration-free human iPSCs have been generated using several methods, including adenovirus[2], Sendai virus[3], the piggyBac system[4], minicircle vector[5], episomal vectors[6], direct protein delivery[7] and synthesized mRNA[8] (**Supplementary Table 1**). However, reprogramming efficiency using integration-free methods is impractically low in most cases. Direct delivery of proteins or RNA is labor-intensive, requiring repeated delivery of the reprogramming factors. Modifying Sendai virus vectors or preparing synthesized RNA are technically demanding.

In the original report describing episomal plasmid vectors for reprogramming, the authors used seven factors, including *POU5F1* (also known as *OCT3/4*), *SOX2*, *KLF4*, *MYC* (also known as *c-MYC*), *NANOG*, *LIN28A* (also known as *LIN28*) and SV40 large T antigen (*SV40LT*), in three different vector combinations[6] (T1–T3 combinations; **Fig. 1a** and **Supplementary Table 2**). In this study, we used two findings from our laboratory to enhance efficiency of reprogramming by episomal plasmids: iPSC generation is markedly enhanced by p53 suppression[9], and L-Myc is more potent and specific than c-Myc during human iPSC generation[10].

We prepared four vector combinations (**Fig. 1a** and **Supplementary Table 2**). The Y1 combination had six factors (*OCT3/4*, *SOX2*, *KLF4*, *c-MYC*, *LIN28* and *NANOG*) in three episomal plasmids. The Y2 combination contained an additional *TP53* (also known as *p53*) shRNA in one of the three plasmids. We replaced *c-MYC* and *NANOG* with *MYCL1* (also known as *L-MYC*) in the Y1 and Y2 combinations, respectively, to yield the Y3 and Y4 combinations (**Fig. 1b**).

We electroporated these seven combinations of episomal vectors (Y1–Y4 or T1–T3) into three human dermal fibroblast (HDF) lines and two dental pulp cell lines on day 0 (**Fig. 1c**). We trypsinized transfected cells on day 7 and reseeded them onto feeder layers. We maintained the cells in embryonic stem cell (ESC) medium, and small cell colonies became visible ~2 weeks after transfection. We counted the number of colonies with a flat human ESC–like morphology and non-ESC-like colonies around day 30 (**Supplementary Fig. 1**). The Y4 combination resulted in significantly ($P < 0.05$) more iPSC colonies than did any of T1–T3 combinations (**Fig. 1d**). In addition to these five parental cell lines, we obtained iPSC colonies from seven additional HDF lines with the Y4 combination of factors (**Supplementary Table 3**).

We expanded ESC-like colonies derived with the Y4 combination for additional experiments. The majority of the colonies were expandable and exhibited a cellular morphology similar to that of human ESCs, characterized by large nuclei and scant cytoplasm (**Fig. 2a**,**b**). We termed these episomal plasmid vector-derived iPSCs 'pla-iPSCs'. Ten of eleven clones we analyzed were karyotypically normal (**Supplementary Fig. 2** and **Supplementary Table 4**). Short tandem repeat analyses confirmed that pla-iPSC clones were derived from HDFs and dental pulp cells (**Supplementary Table 5**). Reverse transcription–PCR (RT-PCR) analyses revealed that pla-iPSC clones expressed pluripotent stem cell markers, such as *OCT3/4*, *SOX2*, *NANOG* and *DPPA5*, at levels comparable to those in ESCs and retrovirus-derived iPSC clones (**Fig. 2c** and **Supplementary Figs. 3a**, **4** and **5**). Global gene expression profiles also showed that pla-iPSC clones were similar to ESC and retro-iPSC clones (**Supplementary Fig. 6** and **Supplementary Table 6**). The DNA methylation levels of CpG sites in the promoter region of *NANOG* were high in parental HDFs and dental pulp cells but were low in pla-iPSCs and ESCs (**Fig. 2d**).

To examine whether episomal vectors persisted in pla-iPSCs, first we transfected an episomal vector encoding enhanced GFP

[1]Center for iPS Cell Research and Application, Kyoto University, Kyoto, Japan. [2]Department of Biological Repair, Institute for Frontier Medical Sciences, Kyoto University, Kyoto, Japan. [3]Laboratory for Retinal Regeneration, Center for Developmental Biology, RIKEN, Kobe, Japan. [4]Department of Tissue and Organ Development, Gifu University Graduate School of Medicine, Gifu, Japan. [5]Department of Oral and Maxillofacial Science, Gifu University Graduate School of Medicine, Gifu, Japan. [6]Human Leukocyte Antigen (HLA) Laboratory, Kyoto, Japan. [7]Institute for Integrated Cell-Material Sciences, Kyoto University, Kyoto, Japan. [8]Yamanaka Induced Pluripotent Stem Cell Project, Japan Science and Technology Agency, Kawaguchi, Japan. [9]Gladstone Institute of Cardiovascular Disease, San Francisco, California, USA. Correspondence should be addressed to K.O. (okita@cira.kyoto-u.ac.jp) or S.Y. (yamanaka@cira.kyoto-u.ac.jp).

RECEIVED 29 OCTOBER 2010; ACCEPTED 8 FEBRUARY 2011; PUBLISHED ONLINE 3 APRIL 2011; DOI:10.1038/NMETH.1591

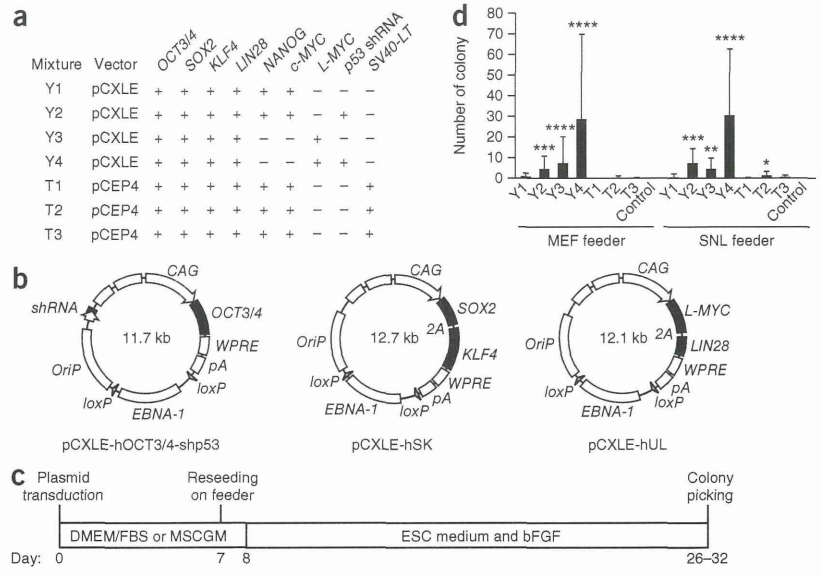


**Figure 1** | Establishment of human iPSCs. (**a**) Combinations of reprogramming factors and episomal vectors used in this study. (**b**) Episomal expression vectors in the Y4 combination. *CAG*, CAG promoter; *WPRE*, woodchuck hepatitis post-transcriptional regulatory element; and *pA*, polyadenylation signal. (**c**) Schematic of the pla-iPSC induction protocol. DMEM, Dulbecco's modified Eagle medium; FBS, fetal bovine serum; MSCGM, mesenchymal stem cell growth medium; bFGF, basic fibroblast growth factor. (**d**) Numbers of colonies per $1.0 \times 10^5$ cells obtained with different combinations of reprogramming factors. Control, cells transduced with episomal vector encoding EGFP; MEF, mouse embryonic fibroblasts; SNL, mouse embryonic fibroblast cell line. Data are means ± s.d. of numbers of ESC-like colonies obtained from 15 independent induction experiments using five cell lines. $^{****}P < 0.05$ against T1, T2, T3 and control; $^{***}P < 0.05$ against T1, T3 and control; $^{**}P < 0.05$ against T1 and control; $^{*}P < 0.05$ against control.

(EGFP) into fibroblasts and monitored fluorescence. Sixty-eight percent of the cells were fluorescent 1 week after transfection (**Supplementary Fig. 7**). However, the signal quickly decreased thereafter, and only 2.4% of cells were fluorescent 4 weeks after electroporation. Then we estimated the copy numbers of the episomal vectors in established pla-iPSC clones. We designed a PCR primer pair for *EBNA-1* sequence derived from Epstein-Barr virus to calculate the copy numbers of the episomal vectors and another primer pair for the endogenous *FBXO15* locus to estimate the cell number. We detected ~200 copies of the episomal vectors per cell 6 d after transfection (**Fig. 2e** and **Supplementary Fig. 3b**). In contrast, we detected no *EBNA-1* DNA in five of seven clones tested at passages 11–20 (~80–120 d after transfection). The remaining two clones contained ~0.001 and 2 copies, respectively. The latter clone likely had integrated the plasmid into a chromosome.

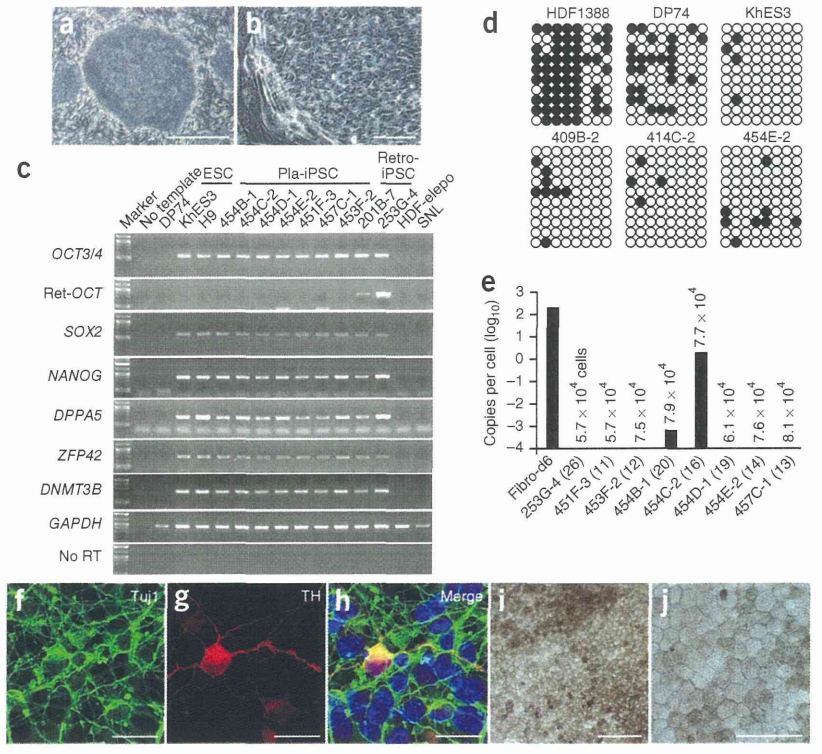


**Figure 2** | Characterization of pla-iPSC clones. (**a**,**b**) Phase contrast images of an established pla-iPSC line. Scale bars, 1 mm (**a**) and 100 µm (**b**). (**c**) RT-PCR analyses for pluripotent cell markers. Total RNA was isolated from pla-iPSC clones established with the Y1 (clone 454B-1), Y2 (454C-2), Y3 (454D-1) or Y4 (454E-2, 451F-3, 457C-1 and 453F-2) combinations, from retrovirus-derived iPSC clones (retro-iPSC) and from ESC lines. In the lanes labeled *OCT3/4* and *SOX2*, PCR primers only detected endogenous gene expression; in the Ret-*OCT* lane, PCR primers specifically amplified the retroviral *OCT3/4* transgene. *GAPDH* was used as a loading control. As a negative control, *GAPDH* amplification was also performed without reverse transcription (no RT). Fibroblasts 4 d after electroporation of the Y4 mixture (HDF-elepo) and mouse embryonic fibroblast cell line (SNL) were used as other negative controls. (**d**) DNA methylation status of the *NANOG* promoter region in the indicated cell lines. Open and closed circles indicate unmethylated and methylated CpG dinucleotides, respectively. (**e**) Copy numbers of episomal vectors in pla-iPSC clones. Numbers in parentheses indicate passage number. Also shown are the estimated numbers of cells analyzed for each clone. Fibroblasts 6 d after electroporation of the Y4 combination were analyzed (fibro-d6) as a positive control. (**f**–**h**) Differentiation of pla-iPSC clone (454E-2) into dopaminergic neurons. Micrographs are immunostained for Tuj1 (**f**) and tyrosine hydroxylase (TH) (**g**). A merged image with nuclear staining using DAPI (**h**) is shown. Scale bars, 20 µm. (**i**,**j**) Differentiation of pla-iPS clone (454E-2) into retinal pigment epithelial cells. Scale bars, 100 µm (**i**) and 50 µm (**j**).

These data demonstrated that the episomal vectors were spontaneously lost in the majority of pla-iPSC clones.

We examined the differentiation potential of pla-iPSCs *in vivo*. Injection of pla-iPSCs into the testes of immunodeficient mice yielded tumors within 3 months. Histological examination confirmed that these tumors were teratomas and contained tissues of all three germ layers, including neural epithelium, cartilage and gut-like epithelium (**Supplementary Fig. 8**).

We carried out directed differentiation of the pla-iPSCs into dopaminergic neurons *in vitro* (Online Methods). RT-PCR detected upregulation of *SOX1*, a marker of immature neural cells, and downregulation of *OCT3/4* 12 d after induction (**Supplementary Fig. 9a**). Immunostaining showed that the majority of cells expressed Nestin after 29 d, with some cells still proliferating and expressed Ki67 (**Supplementary Fig. 9b–e**). Clusters of Nestin-expressing cells expressed PAX6, and more mature cell clusters expressed tyrosine hydroxylase, a marker of dopaminergic neurons (**Supplementary Fig. 9f,g**). Tyrosine hydroxylase–expressing cells localized with the neural markers Tuj1 and MAP2ab, and the vesicular monoamine transporter VMAT2 (**Fig. 2f–h** and **Supplementary Fig. 9h–l**). Therefore, pla-iPSCs have the potential to differentiate into dopaminergic neurons.

We also examined whether pla-iPSC clones differentiated into retinal pigment epithelial cells using a modified stromal cell–derived inducing activity method (Online Methods). Five of six pla-iPSC clones developed pigmented cell clusters after 30 d in conditioning medium of mouse PA6 stromal cells. The clusters grew and exhibited a squamous and hexagonal morphology, characteristic of retinal pigment epithelial cells (**Fig. 2i,j**).

We examined the human leukocyte antigen (HLA) types of our dental pulp-derived iPSC lines. In a previous study only one HLA type had been detected in two dental pulp lines by a PCR–reverse sequence–specific oligonucleotide probe (rSSOP) protocol[11]: line DP74 had been typed as *HLA-A*24*, –; *HLA-B*52*, –; *HLA-DRB1*15*, –, and line DP94 as *HLA-A*11*, –; *HLA-B*15*, –; *HLA-DRB1*04*, – ('–' means no other allele was detected; **Supplementary Table 7**). We also typed these lines with two additional analyses. A PCR-rSSOP protocol optimized for the Japanese population typed line DP74 and its progeny iPSC lines (454E-2 and 457C-1) as *HLA-A*24:02*, –; *HLA-B*52:01*, –; *HLA-DRB1*15:02*, –, and typed DP94 and its progeny iPSC line (453F-2) as *HLA-A*11:01*, –; *HLA-B*15:01*, –; *HLA-DRB1*04:06*, –. Sequence-based typing showed that the types of DP74 and DP94 were *HLA-A*24:02:01*, –; *HLA-B*52:01:01*, –; *HLA-DRB1*15:02:01*, – and *HLA-A*11:01:01*, –; *HLA-B*15:01:01*, –; *HLA-DRB1*04:06:01*, –, respectively. The families of the donors of the two dental pulp lines could not be typed because the lines were established in an anonymous way. Therefore, it is not possible to formally conclude that these donors are homozygous for the HLA haplotypes. Nevertheless, the fact that three independent analyses detected only one type in each donor is indicative of homozygosity.

According to the HLA Laboratory database, frequencies of *HLA-A*24:02*; *HLA-B*52:01*; *HLA-DRB1*15:02* and *HLA-A*11:01*; *HLA-B*15:01*; *HLA-DRB1*04:06* haplotypes in the Japanese population are 8.5% and 1.3%, respectively (http://www.hla.or.jp/hapro_e/top.html; **Supplementary Table 8**). Theoretically, iPSCs established from these two individuals match ~20% of all the combinations of 2,117 haplotypes in Japanese population. Indeed, pla-iPSC lines derived from lines DP74 and DP94 match 32 of 107

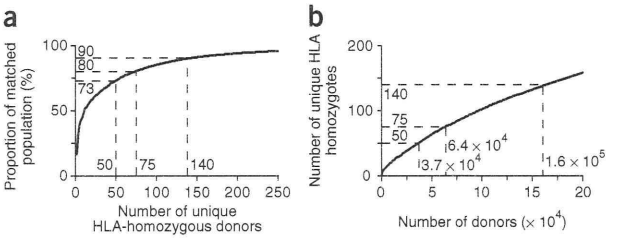


**Figure 3** | Estimated coverage of the Japanese population by HLA homozygous donors. (**a**) Estimated cumulative coverage of the Japanese population by theoretical unique *HLA* homozygous donors at *HLA-A*, *HLA-B* and *HLA-DRB1* loci with four-digit specification. (**b**) Estimated numbers of donors required to identify individuals with unique HLA homozygous haplotypes.

donors[11] at the three *HLA* loci (*HLA-A*, *HLA-B* and *HLA-DR*) with the two-digit specification (**Supplementary Table 7**).

Others previously estimated that iPSC lines with 50 unique HLA homozygous haplotypes would match ~90% of the Japanese population at the *HLA-A*, *HLA-B* and *HLA-DRB1* loci with two-digit specification[12]. We performed a similar estimation with four-digit specification using the HLA Laboratory database and found that 50 unique HLA-homozygous donors would cover ~73% of the Japanese population (**Fig. 3a** and **Supplementary Table 8**). Approximately 75 and 140 unique donors would be needed to cover ~80% and 90%, respectively. It would be necessary to type ~37,000, ~64,000 and ~160,000 individuals, respectively, to identify these 50, 75 and 140 donors (**Fig. 3b**).

Allografts using *HLA*-homozygous iPSCs may provide a therapeutic alternative to autologous grafts, for cases in which transplant is likely to be needed soon after injury; furthermore, they allow for the advance selection of safe clones[13]. The beneficial effects of matching at major *HLA* loci are well documented in renal transplantation[14,15], although recipients of allografts derived from *HLA*-homozygous iPSCs would still need immunosuppressants after transplantation because of other HLA antigens, non-HLA antigens and immunity by natural killer cells.

We report a simple, non-integrative method for reprogramming human cells. The increased efficiency and the use of non-transforming Myc should be useful to generate iPSCs from many donors, such as individuals with disease. The approach may also prove beneficial for generating human iPSCs for use in autologous and allologous stem cell therapy.

## METHODS

Methods and any associated references are available in the online version of the paper at http://www.nature.com/naturemethods/.

**Accession codes.** Addgene: 27076 (pCXLE-hOCT3/4), 27077 (pCXLE-hOCT3/4-shp53-F), 27078 (pCXLE-hSK), 27079 (pCXLE-hMLN), 27080 (pCXLE-hUL), 27081 (pCXLE-Fbx15-cont2) and 27082 (pCXLE-EGFP).

*Note: Supplementary information is available on the Nature Methods website.*

**ACKNOWLEDGMENTS**

We thank K. Takahashi, T. Aoi and Y. Yoshida for scientific discussion; M. Narita, T. Ichisaka, M. Ohuchi, M. Nishikawa and N. Takizawa for technical assistance; R. Kato, E. Nishikawa, S. Takeshima, Y. Ohtsu and H. Hasaba for administrative assistance; and H. Niwa (RIKEN) and J. Miyazaki (Osaka University) for the *CAG* promoter. This study was supported in part by a grant from the Program

for Promotion of Fundamental Studies in Health Sciences of National Institute of Biomedical Innovation, a grant from the Leading Project of Ministry of Education, Culture, Sports, Science and Technology (MEXT), a grant from Funding Program for World-Leading Innovative Research and Development on Science and Technology (FIRST Program) of Japan Society for the Promotion of Science, Grants-in-Aid for Scientific Research of Japan Society for the Promotion of Science and MEXT (to S.Y.) and Senri Life Science Foundation (to K.O.). H.H. is supported by a Japanese government (MEXT) scholarship.

### AUTHOR CONTRIBUTIONS

K.O. and S.Y. conceived the project and wrote the manuscript. K.O. constructed the vectors with H.H., M.N. and K. Tanabe, and conducted most of the experiments with Y.M., Y. S. and A.O. A.M. and J.T. carried out the differentiation experiment into dopaminergic neurons. S.O. and M.T. performed differentiation into retinal pigment epithelial cells. K. Tezuka., T.S. and T.K. established dental pulp cell lines. H.S. performed HLA haplotyping in Japanese population and supervised HLA analysis.

### COMPETING FINANCIAL INTERESTS

The authors declare competing financial interests: details accompany the full-text HTML version of the paper at http://www.nature.com/naturemethods/.

**Published online at http://www.nature.com/naturemethods/.**
**Reprints and permissions information is available online at http://www.nature.com/reprints/index.html.**

1. Okita, K., Ichisaka, T. & Yamanaka, S. *Nature* **448**, 313–317 (2007).
2. Zhou, W. & Freed, C.R. *Stem Cells* **27**, 2667–2674 (2009).
3. Fusaki, N., Ban, H., Nishiyama, A., Saeki, K. & Hasegawa, M. *Proc. Jpn. Acad. B* **85**, 348–362 (2009).
4. Woltjen, K. *et al. Nature* **458**, 766–770 (2009).
5. Jia, F. *et al. Nat. Methods* **7**, 197–199 (2010).
6. Yu, J. *et al. Science* **324**, 797–801 (2009).
7. Kim, D. *et al. Cell Stem Cell* **4**, 472–476 (2009).
8. Warren, L. *et al. Cell Stem Cell* **7**, 618–630 (2010).
9. Hong, H. *et al. Nature* **460**, 1132–1135 (2009).
10. Nakagawa, M., Takizawa, N., Narita, M., Ichisaka, T. & Yamanaka, S. *Proc. Natl. Acad. Sci. USA* **107**, 14152–14157 (2010).
11. Tamaoki, N. *et al. J. Dent. Res.* **89**, 773–778 (2010).
12. Nakatsuji, N., Nakajima, F. & Tokunaga, K. *Nat. Biotechnol.* **26**, 739–740 (2008).
13. Tsuji, O. *et al. Proc. Natl. Acad. Sci. USA* **107**, 12704–12709 (2010).
14. Takemoto, S.K., Terasaki, P.I., Gjertson, D.W. & Cecka, J.M. *N. Engl. J. Med.* **343**, 1078–1084 (2000).
15. Aydingoz, S.E. *et al. Hum. Immunol.* **68**, 491–499 (2007).

## ONLINE METHODS

**Cell culture.** Human fibroblasts HDF1419, HDF1388, HDF1429, HDF1377, HDF1437 and HDF1554 were purchased from Cell Applications, and TIG121, TIG120, TIG114 and TIG107 were obtained from the Japanese Collection of Research Bioresources. Human fibroblasts were cultured in DMEM (Nacalai Tesque) supplemented with 10% FCS (Invitrogen). Human dental pulp (DP) cells were established from human third molars as described previously[11] and were maintained in mesenchymal stem cell growth medium (MSCGM; Lonza). Human ESC lines (KhES-1 and KhES-3) were obtained from Kyoto University. H1 and H9 were from WiCell Research Institute. Mouse embryonic fibroblasts (MEFs) were isolated from embryonic day 13.5 embryos of C57BL/6 mice. All mice used in this study were bred and killed appropriately following code of ethics of animal research committee in Kyoto University. MEF and mouse embryonic fibroblast cell line (SNL) cells[16] were cultured in DMEM supplemented with 7% (v/v) FCS, 2 mM L-glutamine and 50 units and 50 mg $ml^{-1}$ penicillin and streptomycin, respectively. Established iPSCs and ESCs were maintained on mitomycin C–treated SNL cells in primate ESC medium (ReproCELL) containing 4 ng $ml^{-1}$ of bFGF (Wako) as described previously[17].

**Vector construction.** Efficient transgene expression was achieved by inserting the woodchuck hepatitis post-transcriptional regulatory element (*WPRE*) upstream of the polyadenylation signal of pCX-EGFP[18]. The episomal cassette was transferred from pCEP4 (Invitrogen). The *EBNA-1* sequence (EcoRI and MfeI sites) was flanked by two *loxP* sequences, and the *loxP–EBNA-1–loxP–OriP* cassette was then digested with BamHI and BglII and inserted into the BamHI site of pCX-EGFP containing the *WPRE*. This episomal vector was designated pCXLE-EGFP.

Human cDNAs encoding *OCT3/4*, *SOX2*, *KLF4*, *c-MYC*, *L-MYC*, *NANOG* and *LIN28* were amplified by PCR and cloned into pCR2.1 (Invitrogen). The translation termination codons of *SOX2*, *c-MYC*, *L-MYC* or *LIN28* were replaced with a BamHI site and then were also cloned into pCR2.1. The cDNAs without a translation termination codon were thereafter ligated with *2A* self-cleavage sequences in pBS-2A[19] with appropriate restriction enzymes to generate pBS–cDNA–2A. *c-MYC–2A* was digested with NotI and BspHI and was ligated into the NotI and NcoI sites of pBS-LIN28-2A in the same reading frame to generate the *c-MYC–LIN28–NANOG* cassette. These *cDNA–2A* or *c-MYC–2A–LIN28–2A* constructs were then ligated to another cDNA or *NANOG* in pCR2.1 with the translation termination codon in the same reading frame using appropriate restriction enzymes. These cDNA-*2A*-cDNA-stop or *c-MYC–2A–LIN28–2A–NANOG*–stop constructs were then inserted into the EcoRI site of pCXLE-EGFP. pCXLE-hOCT3/4-shp53 was constructed by inserting an shRNA expression cassette for *p53*, driven by the mouse *U6* promoter, into the BamHI site of pCXLE-hOCT3/4. The pCXLE-Fbx15-cont2 was generated by inserting the *FBXO15* cDNA into pCXLE-EGFP. Episomal vectors described previously[6] were obtained from Addgene (20922–20927).

**Generation of iPSCs with episomal vectors.** HDF and DP cells were cultured in DMEM supplemented with 10% FBS and mesenchymal stem cell growth medium (MSCGM), respectively. Three micrograms of expression plasmid mixtures were electroporated into $6 \times 10^5$ HDF or DP cells with Microporator (Invitrogen) with a 100-µl kit according to the manufacturer's instructions. The plasmid mixtures used in the experiments are shown in **Supplementary Table 2**. Conditions used were 1,650 V, 10 ms, 3 time pulses for HDF, and 1,800 V, 20 ms, 1 time pulse for DP cells. The cells were trypsinized 7 d after transduction, and $1 \times 10^5$ cells were re-plated onto 100-mm dishes covered with an SNL or MEF feeder layer. The culture medium was replaced the next day with primate ESC medium containing bFGF. The colonies were counted 26–32 d after plating, and those colonies similar to human ESCs were selected for further cultivation and evaluation. The pla-iPSC clones used in this study are summarized in **Supplementary Table 9**.

**Characterization of pla-iPSC clones.** Isolation of total RNA, RT-PCR of marker gene expression, DNA microarray, bisulfite genomic sequencing and teratoma formation were performed as previously described[17]. The primer sequences used in this study are shown in **Supplementary Table 10**. The chromosomal G-band analyses were performed at the Nihon Gene Research Laboratories. Short tandem repeat analyses were performed at Bex Co.; briefly, genomic DNAs were amplified by the PowerPlex 16 system (Promega) and were then analyzed with an ABI PRISM 3100 genetic analyzer and the GeneMapper v3.5 software program (Applied Biosystems). Differentiation of pla-iPSC clones into dopaminergic neurons was performed using the serum-free culture of embryoid body–like aggregates (SFEB) method combined with double SMAD inhibition by a BMP antagonist and an Activin/Nodal inhibitor as described elsewhere[20]. *In vitro* directed differentiation into retinal pigment epithelial cells was performed with the modified stromal cell–derived inducing activity method[21,22]. Briefly, pla-iPSCs were collected with trypsin and collagenase IV, and were treated with inhibitors for WNT and Nodal signaling under serum-free conditions. The cells were then maintained in PA6-conditioning medium for maturation.

**Episomal copy-number detection.** Cells cultured in 60-mm dishes were collected with a cell scraper after removing feeder cells by treatment with dissociation solution consisting of 0.25% trypsin, 1 mg $ml^{-1}$ collagenase, 1 mM $CaCl_2$ and 20% KSR in PBS. The cells were then placed into tubes and centrifuged, and the cell pellets were lysed with 200 µl of lysis solution, containing 1× Ex Taq buffer (Takara) and 167 µg $ml^{-1}$ proteinase K. The lysates were incubated at 55 °C for 3 h, and proteinase K was inactivated at 95 °C. The lysates were used for quantitative PCR analysis. The pCXLE-hFbx15-cont2 plasmid was used to generate a standard curve to determine the correlation between copy number and threshold cycle (Ct) values for *FBXO15* or *EBNA-1*. Then the copy number of *FBXO15* and *EBNA-1* in each iPSC sample was estimated from the observed Ct values. The cell number in each reaction was estimated by dividing the estimated copy number of *FBXO15* by two since each cell had two *FBXO15* alleles. One reaction included up to $1.2 \times 10^4$ cells. The total copy number of *EBNA-1* was measured in ~$5 \times 10^4$ cells by repeating six or seven reactions.

**HLA typing and estimation of coverage.** HLA typing of 107 DP cell lines was performed with the PCR-reverse sequence specific oligonucleotide probe (rSSOP) method using LABType SSO